

Supplementary Information

Boosting the enzymatic activity of CxxC motif-containing PDI family members

Tsubura Kuramochi,^{a, b†} Yukino Yamashita,^{c†} Kenta Arai,^{d, e} Shingo Kanemura,^a

Takahiro Muraoka^{*c, f} and Masaki Okumura^{*a, b}

^a Frontier Research Institute for Interdisciplinary Sciences, Tohoku University, 6-3 Aramaki-Aza-Aoba, Aoba-ku, Sendai 980-8578, Japan.

^b Department of Molecular and Chemical Life Sciences, Graduate School of Life Sciences, Tohoku University, Sendai, Miyagi 980-8577, Japan.

^c Department of Applied Chemistry, Graduate School of Engineering, Tokyo University of Agriculture and Technology, 2-24-16 Naka-cho, Koganei, Tokyo 184-8588, Japan.

^d Department of Chemistry, School of Science, Tokai University, Kitakaname, Hiratsuka-shi, Kanagawa 259-1292, Japan.

^e Institute of Advanced Biosciences, Tokai University, Kitakaname, Hiratsuka-shi, Kanagawa 259-1292, Japan

^f Kanagawa Institute of Industrial Science and Technology, 3-2-1 Sakato, Takatsu-ku, Kawasaki, Kanagawa 213-0012, Japan.

† These authors contributed equally to this work.

Table of Contents

1. Materials	S2
2. Instrumentation	S3
3. Methods	S4
4. Schematic representation of domain compositions in the PDI family	S6
5. Detection of PDI redox status under redox agents	S7
6. Curve fitting analyses to calculate the redox equilibrium constants	S8
7. Oxidative folding assay in the absence of PDI	S9
8. Kinetic analyses of oxidative folding	S10
9. References	S11

1. Materials

The chemical compounds, pMePySS and pMePySH, were synthesized as described previously¹. The aprotinin (bovine pancreatic trypsin inhibitor, #pro-285) was purchased from ProSpec-Tany TechnoGene Ltd, Ness-Ziona, Israel.

2. Instrumentation

Reversed-phase high-performance liquid chromatography (RP-HPLC) was conducted with the GL7400 HPLC system of GL Sciences (Tokyo, Japan) using the TSKgel Protein C4-300 column of Tosoh Bioscience ($\phi 4.6 \times 150$ mm, Tokyo, Japan) for the BPTI folding assay and the TSKgel ODS-100V 5 μm column (Tosoh Bioscience, Japan) for the proinsulin folding assay².

3. Methods

1) Expression and purification of recombinant proteins: Proinsulin was overexpressed in the *Escherichia coli* strain BL21(DE3) by culturing at 37°C overnight. The cells were lysed in 20 mM Tris-HCl (pH 8.0) using a homogenizer (Sonics and Materials, Newtown, CT, USA). After centrifugation of the homogenized lysate, recombinant proinsulin protein was obtained in the form of inclusion bodies. The inclusion bodies were dissolved in 100 mM Tris-HCl (pH 8.0) containing 8 M urea and 30 mM dithiothreitol at 50°C for 1 h. After centrifugation, the supernatant was loaded onto a COSMOSIL 5C18 column (Nacalai Tesque, Kyoto, Japan), and proinsulin was eluted with 80% CH₃CN in 0.05% trifluoroacetic acid. The eluted samples were further purified by RP-HPLC (GL science, Tokyo, Japan), equipped with a COSMOSIL 5C18-AR-II column (Nacalai Tesque) using a linear gradient of CH₃CN in 0.05% trifluoroacetic acid. Collected fractions were lyophilized. The obtained powder was stored at -30°C until use.

PDIA1, PDIA3, PDIA6, and PDIA15 were overexpressed in BL21(DE3) cells and purified as described previously²⁻⁴.

2) Measurement of redox equilibrium: The redox equilibrium between recombinant PDIs and glutathione or compounds was measured as follows. Each PDI enzyme (0.3 μM) was incubated with 90 μM oxidant (GSSG or pMePySS) and various concentrations of reductant (GSH or pMePySH) at 30°C for 1 h in 50 mM Tris-HCl (pH 7.5) containing 300 mM NaCl. After incubation, trichloroacetic acid (10%) was added to prevent further thiol–disulphide exchange. The precipitated pellet was solubilized in 100 mM Tris-HCl (pH 7.0), containing 1% SDS and 1 mM maleimide PEG-2000. The samples were separated by SDS-PAGE. The ratio of the fully reduced form was quantified and plotted using the ImageJ software (National Institutes of Health, Bethesda, MD, USA) and the Igor Pro program (WaveMetrics, Portland, OR, USA).

3) Oxidative folding assay using BPTI: Native BPTI (10 mg) was dissolved in 100 mM Tris-HCl (pH 8.0, 1 mL) containing 30 mM dithiothreitol and 8 M urea and incubated for 3 h at 50°C. The BPTI reduced and denatured forms were purified by RP-HPLC using an InertSustain C18 column (φ4.6×250 mm, GL science, Tokyo, Japan), and the collected fractions were lyophilized. The obtained powder was stored at -30°C until use.

Reduced and denatured forms of BPTI (30 μM) were incubated with/without 0.3 μM PDIA1 or PDIA6 in 100 mM Tris-HCl (pH 7.5) containing 300 mM NaCl, 360 μM reductant (GSH or pMePySH), and 90 μM oxidant (GSSG or pMePySS) at 30°C. The reaction was quenched with an equivalent volume of 1 M HCl at the indicated time points and BPTI folding intermediates were analyzed by RP-HPLC on a TSKgel Protein C4-300 column (Tosoh Bioscience, Japan) with monitoring at 229 nm. The identities of the resulting peaks were confirmed by MALDI-TOF/MS analysis as described previously^{5, 6}.

4) Proinsulin folding assay: Reduced and denatured proinsulin (5 μM) was incubated with/without 0.5 μM PDIA1 or PDIA6 in 100 mM Tris-HCl (pH 7.5) containing 300 mM NaCl, 360 μM reductant (GSH or pMePySH), and 90 μM oxidant (GSSG or pMePySS) at 30°C. The reaction was quenched with an equivalent volume of 2-aminoethyl methanethiosulfonate (AEMTS) (7 mg mL⁻¹) at 30 min to quench their oxidative folding. Reaction mixtures were analyzed by RP-HPLC on a TSKgel ODS-100V 5 μm column (Tosoh Bioscience, Tokyo, Japan) with monitoring at 220 nm. The identities of the resulting peaks were confirmed by MALDI-TOF/MS analysis as described previously^{5, 6}.

4. Schematic representation of the domain compositions of PDI family members.

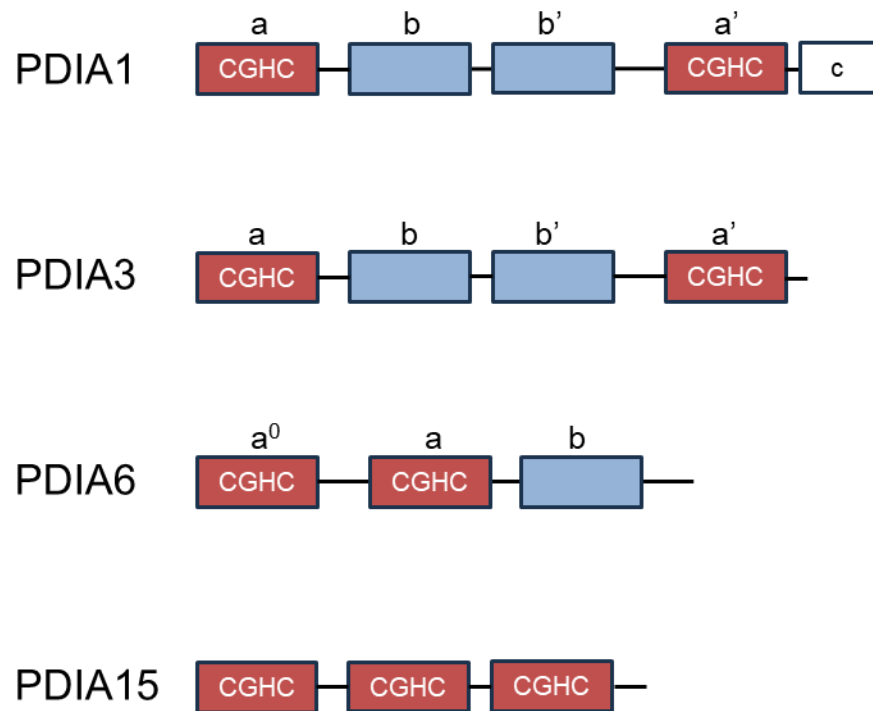
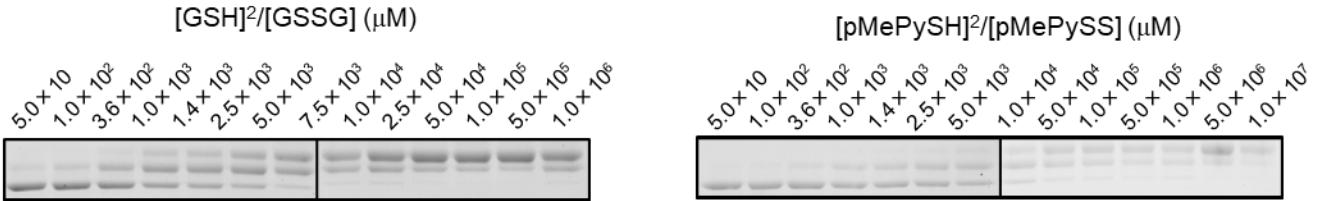


Fig. S1. Schematic representation of the domain compositions of PDI family members.

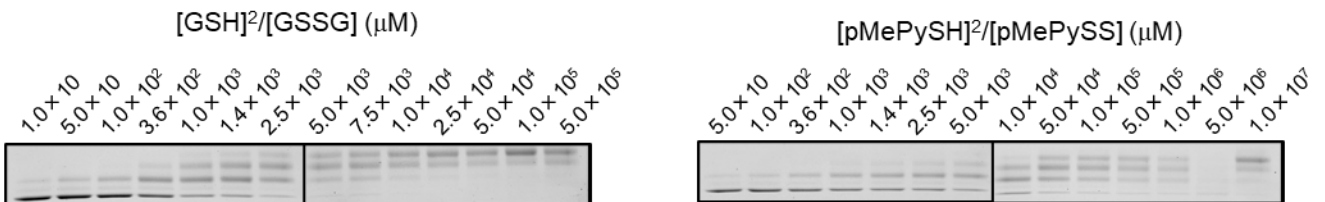
Catalytically active thioredoxin (Trx)-like domains (**a⁰**, **a** or **a'**) are represented in red with active sites indicated; inactive Trx domains are represented in blue (**b** or **b'**); black lines represent linker regions.

5. PDI redox-status detection using redox agents

A) PDIA3



B) PDIA15



C)

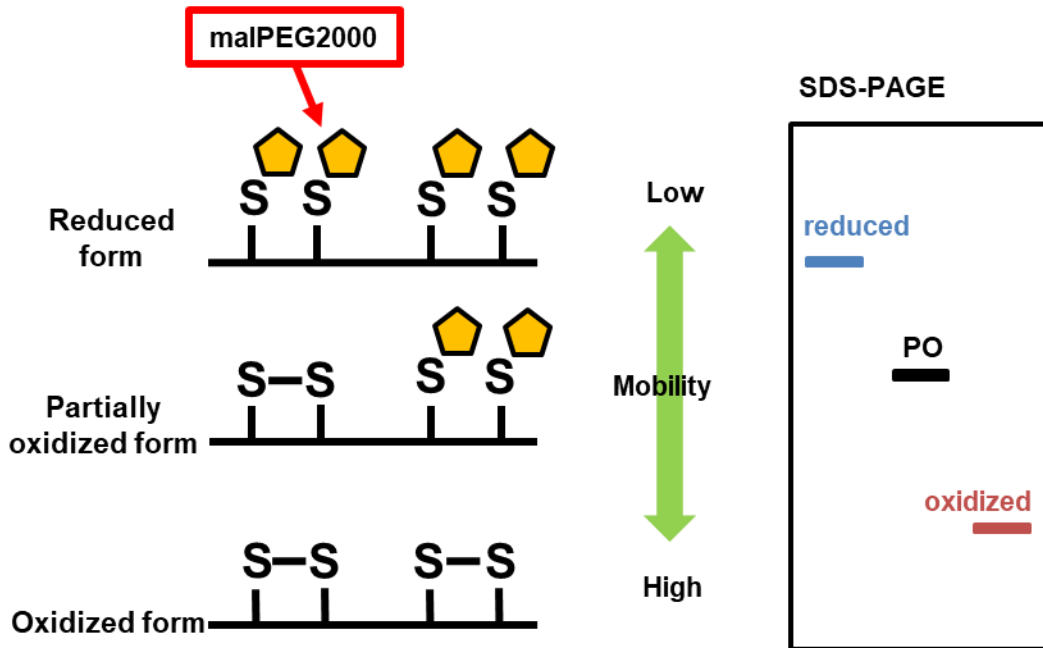
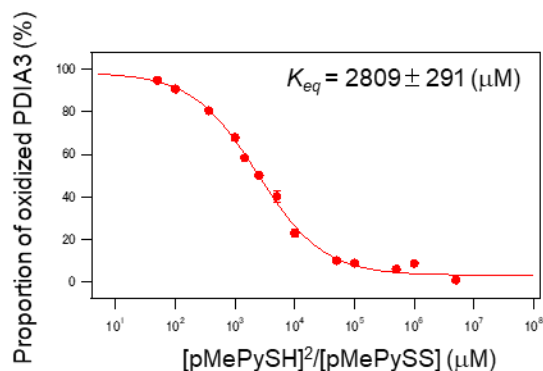
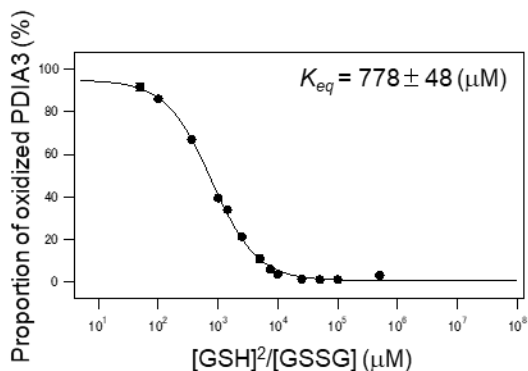


Fig. S2. PDI redox-status detection using redox agents.

Redox states of PDIA3 (A) and PDIA15 (B) using various concentrations of GSH/GSSG or pMePySH/pMePySS. C) schematic diagram of redox detection using non-reducing SDS-PAGE in combination with malPEGE2000.

6. Curve fitting analyses for redox equilibrium constant calculation

A) PDIA3



B) PDIA15

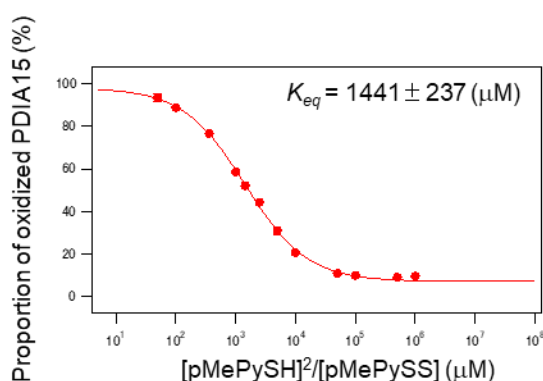
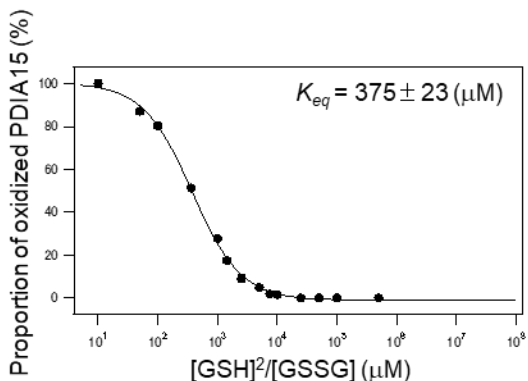


Fig. S3. Curve fitting analyses for redox equilibrium constant calculation.

Proportions of oxidized PDIA3 (A) and PDIA15 (B) are plotted against $[GSH]^2/[GSSG]$ or $[pMePySH]^2/[pMePySS]$ ratios. K_{eq} values were determined from at least three independent experiments (mean \pm SD).

7. Oxidative folding assay in the absence of PDIs

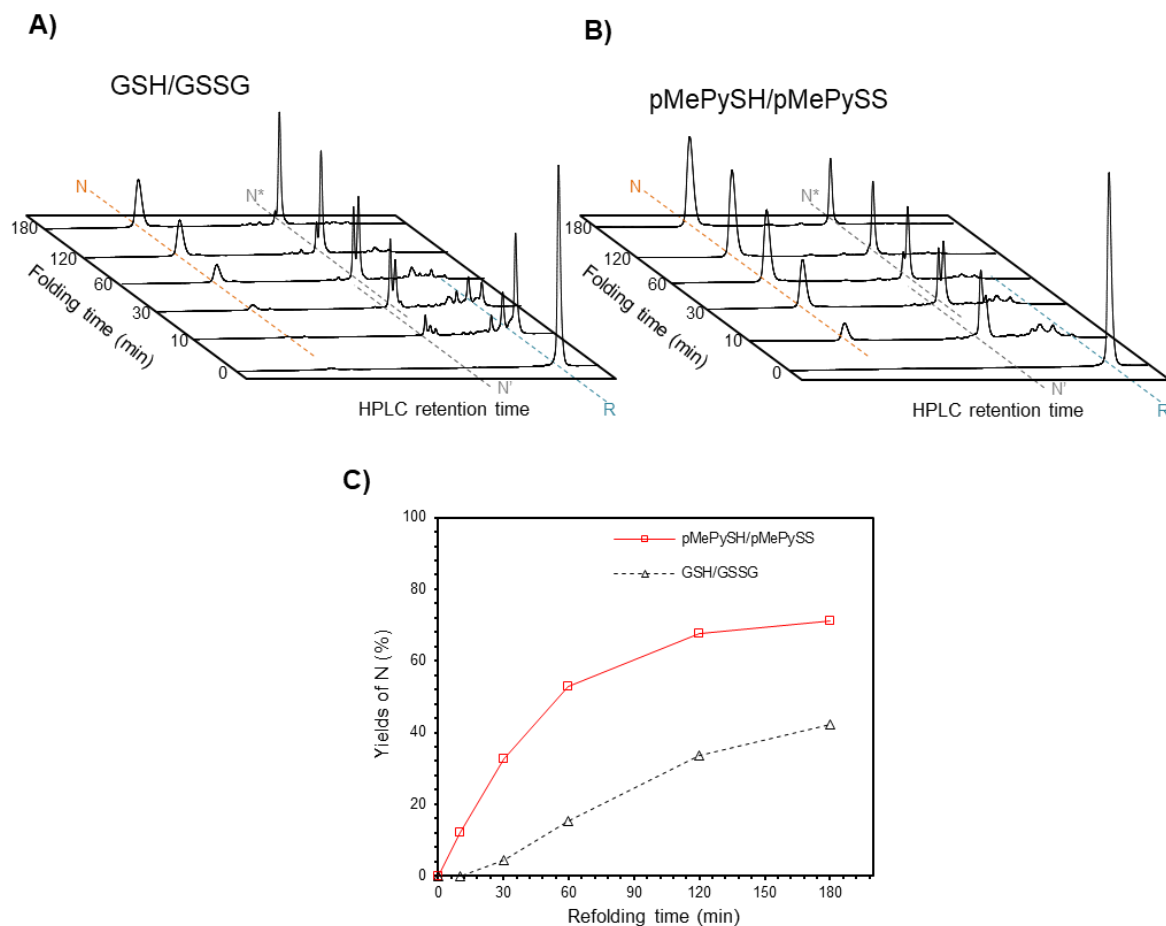


Fig. S4. Oxidative folding assay in the absence of PDIs. Time-course reverse-phase HPLC analyses of oxidative folding of BPTI (30 μM) in the presence of (A) GSH (360 μM)/GSSG (90 μM) and (B) pMePySH (360 μM)/pMePySS (90 μM). N and R represent native and reduced forms of BPTI, respectively. The column was eluted with a gradient consisting of water (containing 0.1% TFA) and CH₃CN (containing 0.1% TFA); flow rate, 1.0 mL min⁻¹; temperature, 30°C. Folding intermediates were analyzed by RP-HPLC on a TSKgel Protein C4-300 column (Tosoh Bioscience, Tokyo, Japan) with monitoring at 229 nm.

8. Kinetic analyses of oxidative folding

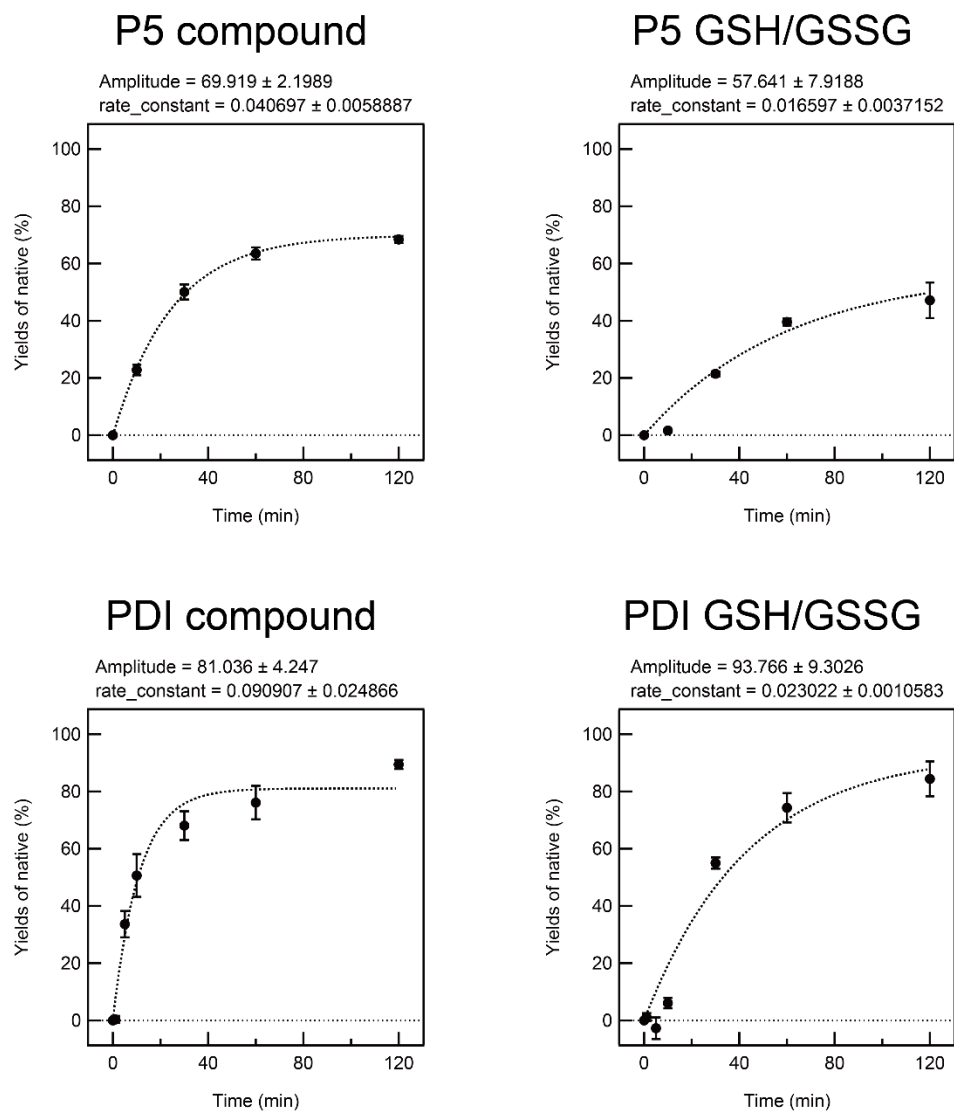


Fig. S5. Kinetic analyses of oxidative folding.

Folding kinetics were determined from the formation rate of native BPTI. The rate constants were determined from at least three independent experiments (mean \pm SD).

9. References

1. S. Okada, Y. Matsumoto, R. Takahashi, K. Arai, S. Kanemura, M. Okumura and T. Muraoka, *Chemical science*, 2023, **14**, 7630–7636.
2. M. Okumura, K. Noi, S. Kanemura, M. Kinoshita, T. Saio, Y. Inoue, T. Hikima, S. Akiyama, T. Ogura and K. Inaba, *Nature chemical biology*, 2019, **15**, 499–509.
3. M. Okumura, S. Kanemura, M. Matsusaki, M. Kinoshita, T. Saio, D. Ito, C. Hirayama, H. Kumeta, M. Watabe, Y. Amagai, Y. H. Lee, S. Akiyama and K. Inaba, *Structure*, 2021, **29**, 1357–1370.e1356.
4. R. Kojima, M. Okumura, S. Masui, S. Kanemura, M. Inoue, M. Saiki, H. Yamaguchi, T. Hikima, M. Suzuki, S. Akiyama and K. Inaba, *Structure*, 2014, **22**, 431–443.
5. M. Okumura, S. Shimamoto, T. Nakanishi, Y. Yoshida, T. Konogami, S. Maeda and Y. Hidaka, *FEBS Lett*, 2012, **586**, 3926–3930.
6. M. Okumura, M. Saiki, H. Yamaguchi and Y. Hidaka, *Febs j*, 2011, **278**, 1137–1144.